Received: 19 March 2023 | Revised: 18 January 2024 | Accepted: 28 January 2024

DOI: 10.1002/cbin.12138

RESEARCH ARTICLE

Cell Biology International WILEY

Epigenetic changes in shear-stressed endothelial cells

Thaís Silva Pinto[1] | Geórgia da Silva. Feltran[1] | Célio Júnior da C. Fernandes[1] | Amanda Fantini de Camargo Andrade[1] | Alex de Camargo Coque[2] | Simone L. Silva[3] | Abdulwahab A. Abuderman[4] | Willian F. Zambuzzi[1] | Rodrigo A. Foganholi da Silva[2,3]

[1]Lab. of Bioassays and Cellular Dynamics, Department of Chemical and Biological Sciences, Institute of Biosciences, Paulista State University—UNESP, Botucatu, São Paulo, Brazil

[2]Epigenetic Study Center and Gene Regulation—CEEpiRG, Program in Environmental and Experimental Pathology, Paulista University, São Paulo, São Paulo, Brazil

[3]School of Dentistry, University of Taubaté, Taubaté, São Paulo, Brazil

[4]Department of Basic Medical Sciences, College of Medicine, Prince Sattam bin Abdulaziz University, Riyadh, Saudi Arabia

Correspondence

Rodrigo A. Foganholi da Silva, Program in Environmental and Experimental Pathology, Paulista University—UNIP, São Paul, Brazil.
Email: dasilasilva.rodrigo.a@gmail.com

Willian F. Zambuzzi, Laboratório de Bioensaios e Dinâmica Celular, Depto. de, Química e Bioquímica Instituto de Biociências—IBB—UNESP, São Paulo, Brazil.
Email: w.zambuzzi@unesp.br

Funding information

Fundação de Amparo à Pesquisa do Estado de São Paulo, Grant/Award Numbers: 2014/22689-3, 2016/01139-0, 2017/18349-0; Conselho Nacional de Desenvolvimento Científico e Tecnológico, Grant/Award Numbers: 314166/2021-1, 301498/2022-9; Coordenação de Aperfeiçoamento de Pessoal de Nível Superior, Grant/Award Number: Code 001

Abstract

Epigenetic changes, particularly histone compaction modifications, have emerged as critical regulators in the epigenetic pathway driving endothelial cell phenotype under constant exposure to laminar forces induced by blood flow. However, the underlying epigenetic mechanisms governing endothelial cell behavior in this context remain poorly understood. To address this knowledge gap, we conducted in vitro experiments using human umbilical vein endothelial cells subjected to various tensional forces simulating pathophysiological blood flow shear stress conditions, ranging from normotensive to hypertensive forces. Our study uncovers a noteworthy observation wherein endothelial cells exposed to high shear stress demonstrate a decrease in the epigenetic marks H3K4ac and H3K27ac, accompanied by significant alterations in the levels of HDAC (histone deacetylase) proteins. Moreover, we demonstrate a negative regulatory effect of increased shear stress on HOXA13 gene expression and a concomitant increase in the expression of the long noncoding RNA, HOTTIP, suggesting a direct association with the suppression of HOXA13. Collectively, these findings represent the first evidence of the role of histone-related epigenetic modifications in modulating chromatin compaction during mechanosignaling of endothelial cells in response to elevated shear stress forces. Additionally, our results highlight the importance of understanding the physiological role of HOXA13 in vascular biology and hypertensive patients, emphasizing the potential for developing small molecules to modulate its activity. These findings warrant further preclinical investigations and open new avenues for therapeutic interventions targeting epigenetic mechanisms in hypertensive conditions.

KEYWORDS

endothelial cell, epigenetics, HOTTIP, HOXA13, hypertension, shear stress

Thaís Silva Pinto and Geórgia da Silva. Feltran contributed equally to this study.

Willian F. Zambuzzi and Rodrigo A. Foganholi da Silva share senior authorship.

1 | INTRODUCTION

Hypertension, characterized by persistently high blood pressure, often stealthily culminates in significant cardiovascular complications before symptoms manifest. This silent progression can lead to atherosclerosis and increased risk of heart attacks and strokes (Expert Panel on Detection, Evaluation, and Treatment of High Blood Cholesterol in Adults, 2001). As a leading cause of mortality worldwide, hypertension is often found intertwined with metabolic abnormalities such as obesity and dyslipidemia, and is a key component of metabolic syndrome as defined by the World Health Organization (Alberti & Zimmet, 1998; Cuspidi et al., 2004; Grundy et al., 2004; Guerrero-Romero & Rodríguez-Morán, 2005; Schillaci et al., 2004). This condition is also of particular concern during pregnancy, where it contributes to a substantial fraction of maternal morbidity and mortality (Bokslag et al., 2016). Recognized as a prime factor in endothelial dysfunction—a cornerstone of vascular pathologies—hypertension calls for an in depth examination of endothelial responses to hypertensive stimuli (Bernatova, 2014).

Shear stress, including laminar and tangential forces exerted by blood flow, is instrumental in regulating gene expression in endothelial cells. This regulation occurs through the activation of mechanosensors and signaling pathways, profoundly impacting endothelial function (Chistiakov et al., 2017). Disruptions to normal shear patterns can lead to alterations in endothelial behavior, underscoring the necessity to expand our knowledge of these mechanisms (Buchanan et al., 2014; Tremblay et al., 2017). In vitro models have provided insights into how abnormal flow patterns, such as low or oscillatory shear stress, can influence the endothelium's critical functions, including its anti-inflammatory and anti-atherosclerotic roles (Cunningham & Gotlieb, 2005). Endothelial cells are central to vascular homeostasis, playing a vital role in blood pressure regulation through their interface with blood flow (Félétou et al., 2010; Fleming, 2010; Iring et al., 2019).

The intricate pathogenesis of hypertension is shaped by a dynamic interplay between genetic predispositions and environmental factors (Simon et al., 2016). Epigenetic processes, including DNA methylation and histone modification, have emerged as significant contributors to vascular dysfunction and the initiation of hypertension (Levy et al., 2017). These mechanisms alter gene expression profiles, impacting transcriptional activity and cellular responses (Delcuve et al., 2009; Lu, 2013). For example, epigenetic modifications of genes like the norepinephrine transporter can enhance autonomic activity, leading to increased blood pressure (Esler et al., 2008), while alterations in the HSD11B2 gene promoter can skew the renin-angiotensin-aldosterone system balance (Udali et al., 2013).

Recent studies have elucidated the role of epigenetic mechanisms, such as histone modifications, in the regulation of genes critical to vascular function and their response to dietary factors like salt (Mu et al., 2011; Pojoga et al., 2011). Furthermore, shear stress itself has been shown to induce epigenetic changes, suggesting a mechanistic link between mechanical forces and gene expression in endothelial cells (Illi et al., 2003; Lee et al., 2012a). The regulation of genes such as ACE1 by histone modifications illustrates the complexity of these epigenetic influences (Lee et al., 2012b), and such modifications have been implicated in the progression of vascular diseases like atherosclerosis (Dong & Weng, 2013; Wierda et al., 2015).

HOXA13, a member of the HOX gene family, is particularly noteworthy for its regulatory influence on vascular development, including vessel branching and adhesion. Understanding its epigenetic regulation could offer breakthroughs in treating vascular disorders (Hrycaj & Wellik, 2016; Shaut et al., 2008b). Despite the recognized importance of epigenetic modifications in hypertension, research on the effects of shear stress under hypertensive conditions is sparse. Developing novel experimental models to study the relationship between epigenetic mechanisms and physiological flow conditions is crucial to expand our knowledge in an experimental animal number reduction perspective. Such advancements could provide key insights into the complex etiology of hypertension, enhancing our understanding of vascular biology and informing new therapeutic strategies.

2 | MATERIALS AND METHODS

2.1 | Reagents

RPMI 1640 Medium, penicillin, streptomycin, and fetal bovine serum (FBS) were obtained from Vitrocell. Bovine serum albumin (BSA), Trizma (Tris), dodecyl sodium sulfate (SDS), glycine, acrylamide, bis-acrylamide, and ammonium persulfate were purchased from Sigma Chemical Co. SYBR Green master mix, TRIzol, DNase I, and High-Capacity cDNA Reverse Transcription Kit were obtained from Life Technologies/Molecular Probes, Inc. Oligonucleotides for gene expression (Table 1) were purchased from Exxtend Solution. Primary and horseradish peroxidase (HRP)-linked secondary antibodies were procured from Cell Signaling Technology, Abcam, and R&D Systems (Table 2). Polyvinylidene difluoride (PVDF) membranes, Chemiluminescence (ECL) Kit, and RC DC™ Protein Assay were obtained from Bio-Rad. All other chemicals and reagents used in this study were of analytical grade and sourced from commercial suppliers.

2.2 | Cell culture and shear stress-induced tensional forces

Immortalized human umbilical vein endothelial cells (HUVECs) (ATCC® CRL-1730™) were cultured in RPMI medium (Vitrocell) supplemented with penicillin (100 U/mL), streptomycin (100 mg/mL), and 10% FBS at 37°C and 5% CO_2. Shear stress-induced tensional forces were applied to the endothelial cells using modified 100 mm culture dishes. A 60 mm culture dish was bonded to the center/bottom of the dish and sterilized under UV light for 15 min, following the method described by dela Paz et al. (2012) (Untergasser et al., 2012) and reproduced by da Silva et al. (2019). The cells were grown until semi-confluence on these modified

TABLE 1 Primer sequences and quantitative polymerase chain reaction cycle conditions for gene expression.

Gene (ID)	Primer	5′–3′ Sequence	Reactions condition	Product size
SETD1A (9739)	Forward	GCG GGC TAT TCT CTC ACT TG	95°C—15s; 60°C—30 s; 72°C—30 s	143 pb
	Reverse	CTT GCA CTG CCA AAT TCT GA		
SUV39H1 (6839)	Forward	GGC AAC ATC TCC CAC TTT GT	95°C—15s; 60°C—30 s; 72°C—30 s	250 pb
	Reverse	CAA TAC GGA CCC GCT TCT TA		
EZH2 (2146)	Forward	AAT CAG AGT ACA TGC GAC TGA GA	95°C—15s; 60°C—30 s; 72°C—30 s	145 pb
	Reverse	GCT GTA TCC TTC GCT GTT TCC		
HAT (8520)	Forward	CAT CCC CAA AGA GTT GAT GG	95°C—10 s; 59°C—30 s; 72°C—30 s	139 pb
	Reverse	GCA GTG GAG AAG AAA CTG GC		
PCAF (8850)	Forward	AAA CCC CCA TTT GAA AAA CC	95°C—10 s; 58°C—30 s; 72°C—30 s	191 pb
	Reverse	TCA GAT CAC GGT GGA TGA AA		
KDM4A (9682)	Forward	TTG CTT GGC ACA CTG AAG AC	95°C—15s; 60°C—30 s; 72°C—30 s	205 pb
	Reverse	TCC AGC CTC TTG AGT CAC CT		
KDM5B (10765)	Forward	CGT GGT TTG GCC TTG TTA GT	95°C—15s; 60°C—30 s; 72°C—30 s	178 pb
	Reverse	ACC ACC CAC AGG TGA AGA AG		
KDM6B (23135)	Forward	CCC CTT CAC ATG GCA GTA GT	95°C—15s; 60°C—30 s; 72°C—30 s	176 pb
	Reverse	GCC TCC TCA CTA TCG TGC TC		
HDAC1 (3065)	Forward	CTG GCC ATC ATC TCC TTG AT	95°C—10 s; 58°C—30 s; 72°C—30 s	216 pb
	Reverse	ACC AGA GAC GTG GAA ACT GG		
HDAC2 (3066)	Forward	TTC TCA GTG CAC CCA GTC AG	95°C—10 s; 59°C—30 s; 72°C—30 s	170 pb
	Reverse	CCA GTA TCC TTG GGG GAA AT		
HDAC3 (8841)	Forward	ACG TGG GCA ACT TCC ACT AC	95°C—10 s; 58°C—30 s; 72°C—30 s	219 pb
	Reverse	GAC TCT TGG TGA AGC CTT GC		
HDAC4 (9759)	Forward	AGT GGC CAG GTT ATC AGT GG	95°C—10 s; 59°C—30 s; 72°C—30 s	176 pb
	Reverse	GGA GAA GAG CCG AGT GTG TC		
HDAC5 (10014)	Forward	CATC TCT GCA GAC CCC TCT C	95°C—10 s; 58°C—30 s; 72°C—30 s	163 pb
	Reverse	CCC ACA CAC TTT CAC CCT CT		
HDAC6 (10013)	Forward	AAG TAG GCA GAA CCC CCA GT	95°C—10 s; 59°C—30 s; 72°C—30 s	416 pb
	Reverse	GTG CTT CAG CCT CAA GGT TC		
HOXA3 (3200)	Forward	ACT AGC CCA GGC AGA GCC	95°C—10 s; 58°C—30 s; 72°C—30 s	374 pb
	Reverse	GTA GGG TTG TTG CTG GCA TT		
HOXA4 (3201)	Forward	GAA GAA GAT CCA TGT CAG CG	95°C—10 s; 58°C—30 s; 72°C—30 s	656 pb
	Reverse	GGA ACT CCT TCT CCA GCT CC		
HOXA6 (3203)	Forward	AAA GCA CTC CAT GAC GAA GG	95°C—10 s; 58°C—30 s; 72°C—30 s	493 pb
	Reverse	CAT GGC TCC CAT ACA CAG C		
HOXA9 (3205)	Forward	AAT GCT GAG AAT GAG AGC GG	95°C—10 s; 58°C—30 s; 72°C—30 s	143 pb
	Reverse	GTA TAG GGG CAC CGC TTT TT		
HOXA13 (3209)	Forward	CCT CTG GAA GTC CAC TCT GC	95°C—10 s; 58°C—30 s; 72°C—30 s	211 pb
	Reverse	GCA CCT TGG TAT AAG GCA CG		
lncRNA HOTTIP (100316868)	Forward	CCT AAA GCC ACG CTT CTT TG	95°C—10 s; 58°C—30 s; 72°C—30 s	142 pb
	Reverse	TGC AGG CTG GAG ATC CTA CT		

(Continues)

TABLE 1 (Continued)

Gene (ID)	Primer	5′–3′ Sequence	Reactions condition	Product size
DNMT1 (1786)	Forward	AGG ACC CAG ACA GAG AAG CA	95°C—15 s; 60°C—30 s; 72°C—30 s	201 pb
	Reverse	GTA CGG GAA TGC TGA GTG GT		
DNMT3A (1788)	Forward	AGG AAG CCC ATC CGG GTG CTA	95°C—15 s; 60°C—30 s; 72°C—30 s	225 pb
	Reverse	AGC GGT CCA CTT GGA TGC CC		
DNMT3B (1789)	Forward	TCG ACT TGG TGG TTA TTG TCT G	95°C—15 s; 60°C—30 s; 72°C—30 s	129 pb
	Reverse	TCG AGC TAC AAG ACT GCT TGG		
TET1 (80312)	Forward	GCC CCT CTT CAT TAC CAA GTC	95°C—15 s; 60°C—30 s; 72°C—30 s	211 pb
	Reverse	CGC CAG TTG CTT ATC AAA ATC		
TET2 (54790)	Forward	GGT GCC TCT GGA GTG ACT GT	95°C—15 s; 60°C—30 s; 72°C—30 s	245 pb
	Reverse	GGA AAA TGC AAG CCC TAT GA		
TET3 (200424)	Forward	GGT CAG GCT GGT TTA CAA CG	95°C—15 s; 60°C—30 s; 72°C—30 s	198 pb
	Reverse	GGC ATA GAC CCA CAC ACA TCT		
GAPDH (2597)	Forward	AAG GTG AAG GTC GGA GTC AA	95°C—10 s; 58°C—30 s; 72°C—30 s	345 pb
	Reverse	AAT GAA GGG GTC ATT GAT GG		
b-actin (60)	Forward	GCA CAG AGC CTC GCC TT	95°C—10 s; 58°C—30 s; 72°C—30 s	253 pb
	Reverse	GTT GTC GAC GAC GAG CG		
18S (100008588)	Forward	CGG ACA GGA TTGACA GAT TGA TAG C	95°C—10 s; 60°C—30 s; 72°C—30 s	118 pb
	Reverse	TGC CAG AGT CTC GTT CGT TAT CG		

Abbreviations: GAPDH, glyceraldehyde 3-phosphate dehydrogenase; lncRNA, long noncoding RNA.

culture dishes and maintained in a humidified atmosphere containing 5% CO_2 at 37°C. The cells were divided into three groups: normotension cultures (Normo) exposed to a rotating frequency of 100 rpm for 24 h, "hypertension" cultures (Hyper) exposed to a rotating frequency of 200 rpm for 24 h, and a return group where the rotating frequency was returned to normotension (100 rpm) for an additional 24 h.

The shear stress was calculated using the equation: $\tau max = \alpha\sqrt{\rho\eta}(2\pi f)^3$, where τmax represents the shear stress (in Pascal), α is the radius of orbital rotation (12 cm − radius of the SK-O180-pro digital orbital shaker), ρ is the density of the cell culture medium (937.5 kg/m^3), η is the viscosity of the cell culture medium (7.5×10^{-4} Pa s), and ƒ is the frequency of rotation. With this calculation, a shear stress of approximately 3 Pa was achieved at a rotating frequency of 100 rpm, which falls within the range of physiological arterial shear stress (approximately 1–4 Pa, Normotension). A rotating frequency of 200 rpm (~9 Pa) was applied to mimic hypertension shear stress conditions in vitro (Cao et al., 2017).

2.3 | Messenger RNA (mRNA) isolation and qPCR

Total mRNA was isolated from three independent experiments using Ambion TRIzol Reagent (Life Sciences, Thermo Fisher Scientific Inc.). Reverse transcription was performed using the High-Capacity cDNA Reverse Transcription Kit (Applied Biosystems) in a thermal cycler (QuantStudio® 3 Real-Time PCR, Thermo Fisher Scientific), following the manufacturer's instructions.

RT-PCR was employed to examine the expression of core constituents involved in histone modifications, DNA methylation, and the *HOXA13* gene in HUVEC cells subjected to a circuit of orbital shear stress-induced tension forces. Real-time PCR was performed using PowerUpTM SYBR™ Green Master Blend (Applied Biosystems). The relative expression levels of specific genes (listed in Table 1) were normalized using a combination of three reference genes (*18S*, *β-ACTIN*, and *GAPDH*) employing the $\Delta\Delta^{CT}$ method. The normotension group (Normo) served as the reference group for comparison.

2.4 | Analysis of 5-methylcytosine (5-meC) and 5-hydroxymethylcytosine (5-hmeC) content

The genomic DNA for analysis of 5-meC and 5-hmeC content on the *HOXA13* gene promoter was purified from three independent experiments using phenol/chloroform/isoamyl alcohol extraction. The concentration of the genomic DNA was measured using the Nanodrop ND-1000. To distinguish between DNA methylation and hydroxymethylation, the genomic DNA was treated with T4-β-glucosyltransferase (T4-BGT) (New England Biolabs), which adds a glucose moiety to 5-hmeC (genomic DNA [gDNA]). For each sample,

TABLE 2 Antibodies used in the study.

Antibody	Code	MW (kDa)		Research
Primary antibodies				
H3K4me3	#9751	17	Rabbit IgG	Cell Signaling Tecnology
H3K9me3	#13969	17	Rabbit IgG	Cell Signaling Tecnology
H3K27me3	#9733	17	Rabbit IgG	Cell Signaling Tecnology
H3K9ac	#9649	17	Rabbit IgG	Cell Signaling Tecnology
H3K27ac	#8173	17	Rabbit IgG	Cell Signaling Tecnology
H3	#4620	17	Rabbit IgG	Cell Signaling Tecnology
SET1	#61702	300	Rabbit IgG	Cell Signaling Tecnology
HAT1	SAB4503405	49	Rabbit IgG	Cell Signaling Tecnology
SUV39	#8729	48	Rabbit IgG	Cell Signaling Tecnology
EZH2	#5246	98	Rabbit IgG	Cell Signaling Tecnology
PCAF	#3378	93	Rabbit IgG	Cell Signaling Tecnology
HDAC1	#5356	62	Mouse IgG1	Cell Signaling Tecnology
HDAC2	#5113	60	Mouse IgG1	Cell Signaling Tecnology
HDCA3	#3949	49	Mouse IgG2a	Cell Signaling Tecnology
p-HDAC	#3443	–	Rabbit IgG	Cell Signaling Tecnology
KDM4A	#5328	–	Rabbit IgG	Cell Signaling Tecnology
KDM5B	#3273	–	Rabbit IgG	Cell Signaling Tecnology
KDM6B	#3457	–	Rabbit IgG	Cell Signaling Tecnology
HOXA13	ab172570	40	Rabbit IgG	Abcam
GAPDH	#5174	37	Rabbit IgG	Cell Signaling Tecnology
Secondary antibodies				
Anti-Mouse—Alexa Fluor 594		–	IgG	Invitrogen/Molecular Probes
Anti-Rabbit—Alexa Fluor 594		–	IgG	Invitrogen/Molecular Probes
Anti-Mouse—HRP	#7076	–	IgG	Cell Signaling Tecnology
Anti-Rabbit—HRP	#7074	–	IgG	Cell Signaling Tecnology

Abbreviations: HRP, horseradish peroxidase; IgG, immunoglobulin G.

three tubes containing 400 ng of gDNA were treated with 1X NE buffer, 40 mM UDP glucose, and T4-BGT (1 unit) to a final volume of 40 µL. The samples were incubated at 37°C for 1 h, followed by 10 min at 65°C. Subsequently, the samples were digested with MspI or HpaII restriction enzymes (New England BioLabs), or H_2O (control) according to the manufacturer's instructions.

Following digestion, gene-specific methylation analysis was performed in a total volume of 10 µL, comprising PowerUp™ SYBR™ Green Master Mix 2x (5 µL) (Applied Biosystems), 0.5 µM of each primer, treated gDNA, and nuclease-free H_2O. The primer sequences (F: 5′-AGTACATTTGGCCGTTCCAG-3′; R: 5′-CTTCTACCACCAGGG CTACG-3′) were designed on regulatory regions such as DNaseI hypersensitivity clusters sites, layered by histone modification marks, CpG regions, and transcription factor binding sites. Primer design and analysis software, along with secondary structure analysis and annealing temperature determination, were performed using the Beacon Designer, Free Edition (http://www.premierbiosoft.com/) (Yoon et al., 2006). The sequences and chromosome location were confirmed using in silico PCR (https://genome.ucsc.edu/). The data were expressed as the percentage of the mean ± standard ratio between 5-meC and 5-hmeC marks obtained from three independent experiments.

2.5 | Western blot

Following the circuit of orbital shear stress-induced tension forces, HUVECs were washed with ice-cold phosphate buffered saline (PBS). Protein extracts were obtained from three independent experiments using RIPA lysis buffer (Sigma Aldrich Co.) supplemented with protease inhibitors (Sigma Aldrich Co.) for 1 h on ice. The protein extracts were then cleared by centrifugation at 13,000*g* for 15 min at

4°C, and the supernatant was stored on ice. The protein concentrations were determined using the Lowry protein assay (McCabe et al., 2012). An equal volume of 2x SDS gel loading buffer (100 mM Tris-HCl, pH 6.8, 200 mM β-mercaptoethanol, 4% SDS, 0.1% bromophenol blue, and 20% glycerol) was added to the protein samples, which were then boiled for 5 min. Equal amounts of protein (75 µg) were loaded onto SDS-PAGE and transferred onto PVDF membranes (Millipore).

The membranes were blocked in 2.5% fat-free dried milk in Tris-buffered saline (TBS) with 0.05% Tween 20 (TBST) and incubated overnight at 4°C with the appropriate primary antibodies (refer to Table 2). After washing with TBST, the membranes were incubated with the appropriate HRP-linked secondary antibodies at a dilution of 1:5000 in the blocking buffer for 1 h. Immunoreactive bands were detected using an enhanced chemiluminescence kit.

2.6 | Laser scanning confocal microscopy

For confocal microscopy analysis, glass coverslips were positioned in the peripheral area of modified 100-mm culture dishes and sterilized under UV light for 15 min. After the orbital shear stress-induced tension forces protocols, the cells were washed with PBS, fixed in 4% paraformaldehyde in PBS, and permeabilized with PBS containing 0.2% Triton-X 100 and 1% BSA at 37°C for 30 min. The cells were then incubated with specific primary antibodies at the recommended concentration by the manufacturer for 1 h. After washing with PBS to remove the primary antibodies, the cells were stained with Alexa Fluor 594 anti-rabbit or mouse immunoglobulin G antibody (Invitrogen/Molecular Probes) for 1 h for fluorescence analysis. Subsequently, the cells were washed, and the coverslips were mounted on glass slides using Fluorosield with 4′,6-diamidino-2′-phenylindole dihydrochloride (DAPI) (Sigma Aldrich Co.).

The stained cells were visualized using an inverted laser scanning confocal microscope (Leica TCS SP5). The acquired images were analyzed using the LAS AF program to determine the intensity of nuclear fluorescence. The nuclear area was initially delimited in a grid acquired from the blue fluorescence channel of the nuclear probe (DAPI). The LAS AF program then determined the intensity of red fluorescence within the restricted area of the nuclear bars. This allowed the relative assessment of protein staining by measuring the intensity of red fluorescence. The data were expressed as the average ± standard deviation of nuclear area fluorescence intensity (red fluorescence) from all cells in the field of view in three independent experiments.

2.7 | Statistical analysis

All experiments were conducted independently at least three times, and the results were presented as the mean ± standard deviation. Statistical analysis was performed using GraphPad Prism 7 software (GraphPad Software). The analysis of variance test with appropriate Bonferroni's correction posttest was applied for parametric data, while nonparametric analysis was utilized for nonparametric data. A *p*-value of less than .05 was considered statistically significant, representing a two-sided test of significance. Densitometric analysis of blots was performed using ImageJ software, and fluorescence intensity was analyzed using the LAS AF program.

3 | RESULTS

3.1 | Chromatin modifications in response to laminar shear stress

Endothelial cells exhibit chromatin remodeling and histone modifications when exposed to shear stress (Wierda et al., 2015). This study sought to discern the influence of shear stress on chromatin structure by quantifying the levels of histone lysine modifications, particularly trimethylation at lysine 4 and 9 (H3K4me3, H3K9me3) and acetylation at lysine 9 and 27 (H3K9Ac, H3K27Ac). Our findings indicate a significant decrease in H3K4me3 and H3K9me3 in the Hyper and Return groups relative to the Normo group (Figure 1a–d). In contrast, H3K27me3 levels did not differ significantly (Figure 1c), suggesting that this histone mark is not substantially altered by shear stress. A noteworthy reduction in acetylation at lysine positions 9 and 27 was also evident in both the Hyper and Return groups (Figure 1n–p). Table 3 delineates the separate effects of histone acetylation and methylation marks examined in our study, and succinctly describes the influence of Laminar Shear Stress on gene expression regulation.

For a deeper understanding of the mechanisms at play, we investigated methyltransferases modifying histone H3 at lysine 4 and 9. SET1A is associated with methylation at lysine 4, leading to various methylation states (Verreault et al., 1998), while SUV39 specifically trimethylates lysine 9 (Du et al., 2017). EZH2, part of the PRC2/EED-EZH2 complex, methylates "Lys-9" and "Lys-27," impacting transcriptional repression (Johnstone, 2002). We measured the expression and protein levels of SET1A, SUV39, and EZH2 in endothelial cells under shear stress. Intriguingly, the transcript levels of SET1A and SUV39 were elevated in the Hyper group compared to the Normo group (Figure 1e). Only SUV39 transcripts were increased in the Return group (Figure 1h). Immunoblotting displayed an augmentation in SET1A (Figure 1f,g) and SUV39 (Figure 1i,j) proteins in the Return group, while a decrease in SUV39 protein was observed in the Hyper group. For EZH2, a modest upsurge in gene expression was noted in the Hyper group (Figure 1k), with a concomitant reduction in protein content for both the Hyper and Return groups as opposed to the Normo condition (Figure 1l,m).

Subsequent analysis show a diminished protein levels of H3K9ac and H3K27ac in both the Hyper and Return groups (Figure 1n–p). Focusing on HAT1, known for acetylating new histones in the cytoplasm (de Ruijter et al., 2003), and PCAF1, a HAT with activity similar to HAT1 (Huynh & McKinsey, 2006), we noted a significant transcript reduction for both in the Return group (Figure 1q,r).

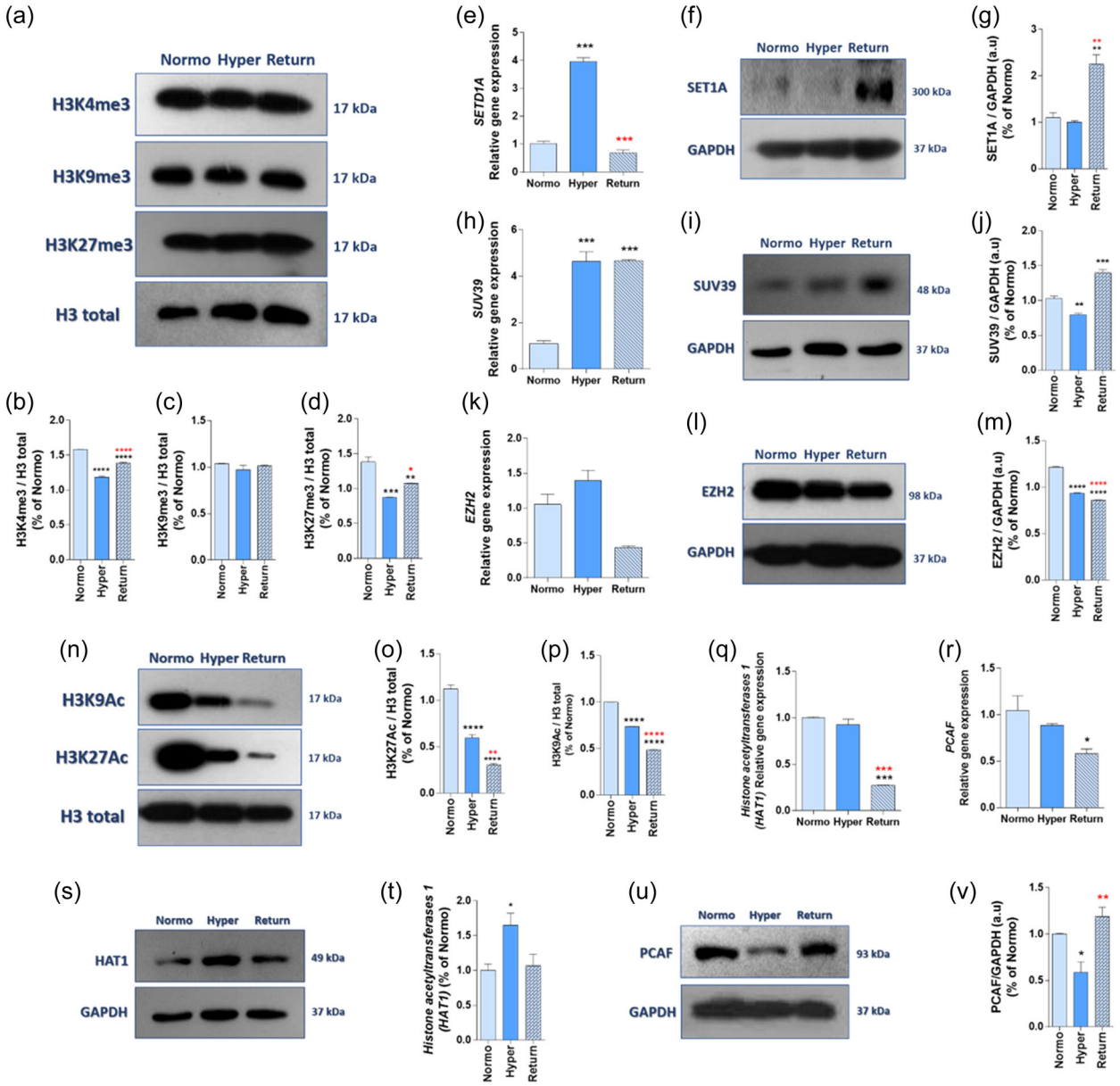

FIGURE 1 Chromatin-modifying metabolism genes and histone lysine modification profile in response to shear stress intensities. Equal amounts of total protein (50 µg) from cell lysates were loaded per lane and subjected to immunoblotting using specific antibodies. A representative immunoblot from three independent experiments is shown, and densitometric analysis was performed to determine the relative intensity ratio of histone 3 methylation and acetylation marks to total histone 3, as well as the protein content ratio to GAPDH. The results demonstrate variations in the trimethylation profile of histone 3 (H3) at lysine 4, 9, and 27 (a–d), as well as the acetylation levels at lysine 9 and 27 (n–p). The constituents involved in these processes at the specific sites of histone 3 (H3), namely SET1A, SUV39, and EZH2, exhibited distinct differences in both gene and protein expression levels among the groups (e–m). The enzymes involved in the rapid acetylation of newly synthesized cytoplasmic histones, HAT1 and PCAF, exhibited varied protein content outcomes but showed similar patterns in gene expression results (q–v). Gene expression was determined by qPCR analysis, normalized to the expression levels of 18S, β-ACTIN, and GAPDH genes, and presented as the mean ± standard deviation of three independent experiments conducted in technical duplicate. The value for the Normo condition was set as 1 and the relative values obtained for the Hyper or Return groups are presented as fold-changes. Statistical significance was determined as $^{*}p < .04$, $^{**}p < .001$, $^{***}p < .0002$, $^{****}p < .0001$ when compared to the control (Normo) group, and $^{*}p < .04$, $^{**}p < .001$, $^{***}p < .0002$, $^{****}p < .0001$ when compared to the Hyper group. EZH2, enhancer of zeste 2 polycomb repressive complex 2 subunit; GAPDH, glyceraldehyde-3-phosphate dehydrogenase; HAT1, histone acetyltransferase 1; H3K4me3, Tri-methylation of lysine 4 on histone H3; H3K9me3, Tri-methylation of lysine 9 on histone H3; H3K27me3, Tri-methylation of lysine 27 on histone H3; H3 total, Total histone 3; H3K9Ac, Acetylation of lysine 9 on histone H3; H3K27Ac, acetylation of lysine 9 on histone H3; PCAF, lysine acetyltransferase 2B; SETD1A, SET domain containing 1A, histone lysine methyltransferase; SUV39, suppressor of variegation 3–9 homolog 1.

TABLE 3 Description of biological effects observed on histone acetylation and methylation marks found in this study.

Histone modifications marks	Impact on gene expression	Laminar shear stress Impact on gene expression	
Methylation		**Hyper**	**Return**
H3K4me3	Promotes gene activation	Reduced	Return to normal
H3K9me3	Promotes activation and silencing	Reduced	Reduced
H3K27me3	Promotes gene silencing	Unchanged	Unchanged
Acetylation			
H3K9Ac	Promotes gene activation	Reduced	Reduced
H3K27Ac	Promotes gene activation	Reduced	Reduced

Protein analysis yielded contrasting results, with an increase in HAT1 and a decrease in PCAF1 in the Hyper group (Figure 1s–v).

3.2 | Oscillatory shear stress and its impact on histone deacetylases: Expression, subcellular localization, and activation

Histone deacetylases (HDACs), crucial for transcriptional regulation, cell cycle progression, and development, remove acetyl groups from lysine residues on core histones, leading to epigenetic repression (Accari & Fisher, 2015). We examined the expression of HDACs in endothelial cells under various shear stress conditions. Quantitative PCR revealed that both class I HDACs (HDAC 1–3) and class II HDACs (HDAC 4–6) were upregulated due to shear stress. Elevated transcription levels of HDACs 2, 3, 4, 5, and 6 were observed in the Hyper group, indicating a pronounced response to increased shear stress. In the Return group, HDACs 1, 2, 4, and 6 also showed increased transcription, with HDACs 3 and 5 presenting more modest, yet still significant, changes (Figure 2a–f). Western blotting confirmed these findings, indicating a slight rise in HDAC1 and a more pronounced increase in HDAC2 protein levels, while HDAC3 levels decreased in the Return group (Figure 2g–l). Phosphorylation, known to regulate HDAC activity and localization (Myers et al., 2000; Zhong et al., 2003), was investigated using confocal microscopy, revealing enhanced nuclear translocation of phosphorylated HDAC (p-HDAC) as seen by the distinctive violet color where nuclear blue fluorescence (DAPI) overlapped with red fluorescence of p-HDAC (Figure 2m). Quantitative analysis with LAS AF programs, after defining nuclear areas based on DAPI staining, confirmed increased nuclear p-HDAC intensity in response to shear stress and in the Return group (Figure 2n).

3.3 | Modulation of histone demethylase activity in response to shear stress

To understand the functional roles of proteins, particularly in nuclear contexts, we investigated the subcellular localization of histone demethylase family members with specific substrate affinities. We selected KDM4A (JMJD2A) targeting H3K9me3, KDM5B (JARID1B) for H3K4me3, and KDM6B (JMJD3) for H3K27me3 (Qin et al., 2010). Gene expression analysis showed that JMJD2A increased in the Hyper group but decreased in the Return group (Figure 3a). JARID1B expression was significantly reduced in both Hyper and Return groups (Figure 3g), while JMJD3 increased in these groups compared to normotensive controls (Figure 3n). Immunofluorescence revealed nuclear localization for KDM4A, with KDM5B and KDM6B found in both the nucleus and cytoplasm (Figure 3b,c, 3h,i, 3o,p). KDM5B had notable nuclear colocalization in the Hyper group (Figure 3h,i), and KDM6B in the Return group (Figure 3o,p), indicating an increase in nuclear KDM protein content in response to shear stress. Pearson correlation analysis revealed a significant inverse relationship between histone methylation marks and nuclear KDM content, with correlation coefficients indicating the strength of these relationships (Figure 3d–f, 3j, 3l,m, 3q–s). To further comprehend the dynamics of KDMs, we assessed the actions of histone methyltransferases SUV39, SET1A, and EZH2, which interact with H3K9me3, H3K4me3, and H3K27me3, respectively. Comparing the nuclear content of histone demethylases to histone methyltransferases revealed a dominance of demethylase activity in endothelial cells under high shear stress (Hyper), suggesting an enhanced demethylation process in these conditions, contributing to the observed changes in histone methylation patterns (Figure 3t–v).

3.4 | HOXA13 involvement in endothelial cells subjected to high shear stress

The role of the HOXA gene cluster, notably in angiogenesis and tissue repair postinjury, is well-established (Baubec & Schübeler, 2014; Jenuwein & Allis, 2001). We probed the function of these homeobox genes under hypertensive conditions by subjecting endothelial cells to high shear stress and evaluating the expression of the HOXA cluster through quantitative PCR. Our observations disclosed varied gene expression within the cluster: HOXA4

expression escalated (Figure 4b), whereas HOXA6 slightly declined in cells recovering to normotensive conditions (Return group) (Figure 4c). Remarkably, HOXA3 expression surged in the Hyper group, with significant decreased for HOXA9 (Figure 4a and 4d). Of particular note, HOXA13 gene and protein expression diminished in cells under high shear stress but increased significantly when conditions returned to normal (Figure 4e–g).

A parallel profile emerged for the long noncoding RNA, lncHOTTIP, which decreased expression under high shear stress but increased in the Return group (Figure 4h). This parallel repression of

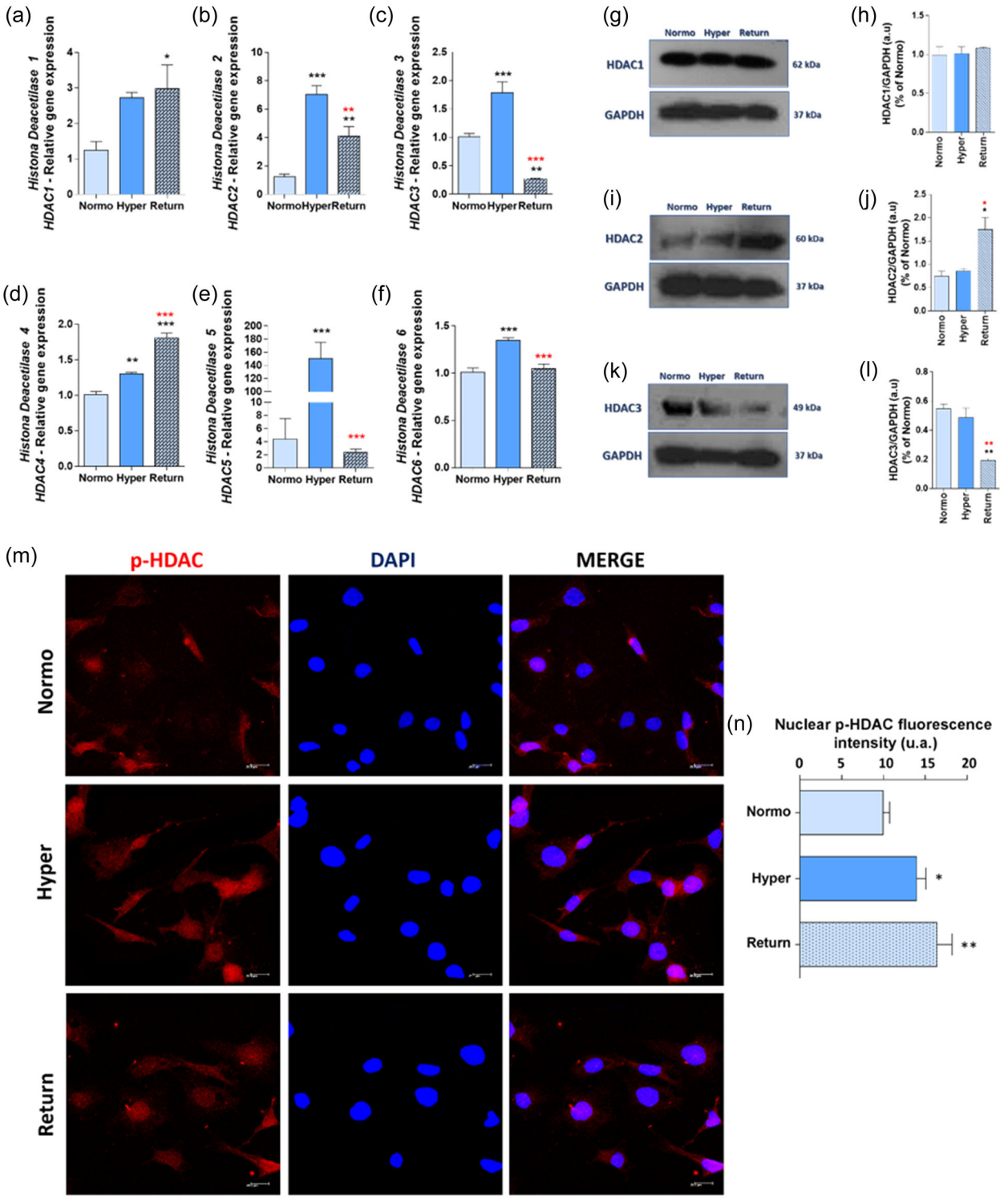

FIGURE 2 (See caption on next page).

lnc-HOTTIP and HOXA13 under stress conditions underscores their potential significance in hypertension etiology, meriting further exploration. These results may offer novel insights into the mechanisms at play and potential therapeutic avenues.

Delving into the epigenetic aspects of HOXA13, we assessed the DNA methylation status of its promoter region alongside DNMT gene expressions. We detected reduced mRNA levels of DNMT1, DNMT3A, and DNMT3B in the Return group, suggesting shifts in DNA methylation dynamics (Figure 4i–k). Interestingly, an elevated expression of DNMT3B mRNA was observed uniquely within the Hyper group, suggesting a specialized regulatory mechanism exclusive to this DNMT isoform. Focusing on the demethylases, an examination of TET2 and TET3 regulation revealed that TET2 mRNA levels were notably increased in the Return group, whereas TET3 mRNA exhibited a decrease. This differential expression underscores a complex regulation of epigenetic modulators in response to variable shear stress conditions. Conversely, TET3 mRNA levels were amplified in the Hyper group (Figure 4l–n). Figure 4o depicts how histone modifications can modulate DNMT activity, potentially activating or inhibiting it. Our methylation analysis of the HOXA13 promoter uncovered significant hypomethylation in cells under high shear stress (Hyper), with a hypermethylation pattern observed upon returning to normotensive conditions (Figure 4p–s).

Importantly, HOXA13's expression does not appear to trigger apoptotic cell death pathways nor suppress endothelial function. This is corroborated by the marked upregulation of the VEGF gene in both Hyper and Return cultures (Figure S1c), indicative of the maintenance of a proliferative endothelial phenotype. Additionally, no changes were noted in the proapoptotic Bax gene expression (Figure S1a), while the antiapoptotic Bcl2 gene saw a notable increase in the Hyper group (Figure S1b). To interrogate the interplay between histone H3 posttranslational modifications and HOXA13 expression, we conducted a Pearson's correlation analysis (Figure 5). This analysis aimed to delineate the association between histone modification levels and HOXA13 expression. We found significant correlations for both acetylation (Figure 5a,b) and methylation (Figure 5c,d) marks, with an inverse relationship noted in the Hyper group in contrast to the direct correlations in the Return group relative to HOXA13 expression.

Summarizing, the data underscore the significant influence of histone modifications on the behavior of the HOXA13 gene in endothelial cells responding to shear stress, indicating that these epigenetic modifications are integral to the mechanosignaling pathway.

4 | DISCUSSION

Endothelial cells are uniquely positioned at the interface between blood flow and vascular tissue, serving as a barometer for changes in hemodynamic forces, particularly under pathophysiological conditions such as hypertension (Chistiakov et al., 2017; Illi et al., 2003). Despite advances in our understanding, the molecular nuances of endothelial mechanosignaling remain partially elucidated. Our prior work has contributed to this knowledge base, revealing the role of c-Src kinase in mechanotransduction via a heat shock protein 70-mediated process and uncovering lnc-HOTAIR as a mechanosensitive gene (Gomes et al., 2020; Pinto et al., 2019; da Silva et al., 2020). These findings have informed our exploration into the epigenetic landscape of mechanosignaling, particularly emphasizing the HOXA cluster genes and the potential role of lnc-HOTTIP, thereby broadening our insights into both developmental biology and hypertension (Shuai et al., 2016).

Histone modifications, as key epigenetic modulators, orchestrate the transcriptional responsiveness of endothelial cells to mechanical stimuli (Jenuwein & Allis, 2001; Narlikar et al., 2002). Our in vitro model simulating these forces has enabled a detailed examination of the impact of shear stress on histone acetylation and methylation. We identified significant epigenetic alterations in endothelial cells under both elevated shear stress (Hyper) and subsequent return to normal conditions (Return), revealing a dynamic epigenetic response to fluctuating mechanical environments.

The interplay between histone acetylation and gene activity is well-established, with HATs and HDACs modulating chromatin

FIGURE 2 Changes in protein and gene expressions of histone deacetylases, likewise in subcellular localization and its activation. Gene expression of HDAC1 to HDAC6 (a–f) was measured by qPCR and normalized to 18S, β-ACTIN, and GAPDH expression levels. The results were expressed as mean ± standard of three independent experiments performed in technical duplicate. One representative immunoblot of three independent experiments is presented (g, i, k) and densitometric analysis are expressed as the relative intensity ratio of GAPDH (h, j, l) revealed protein content changes of HDAC 1, 2 and 3 mainly in Return group. Images of fluorescence confocal microscopy are representative of three independent experiments and show the phosphorylated form of HDAC (p-HDAC) protein subcellular location (m) and the intensity of nuclear fluorescence was determined using a LAS AF program (n). To infer the histone deacetylases activity, the ratio between the nuclear content of the active form of HDACs deacetylases, p-HDAC was shown by the total protein content obtained by the immunoblot of HDACs deacetylases 1, 2 and 3 (o–q) and also the results obtained by the Person's correlation analyzes between the histone deacetylases activity (p-HDAC/HDAC total content) and the global levels of acetylation of the H3K9ac and H3K27ac marks (r–w). The value for Normo condition was normalized to 1 and the relative values obtained to Hyper or Return are shown in fold-changes. Differences were considered statistically significant when $^{*}p < .04$, $^{**}p < .001$, $^{***}p < .0002$, $^{****}p < .0001$ when compared with the control (Normo) group; and $^{*}p < .04$, $^{**}p < .001$, $^{***}p < .0002$, $^{****}p < .0001$ when compared with Hyper group. DAPI, 4′,6-diamidino-2-phenylindole dihydrochloride; GAPDH, glyceraldehyde-3-phosphate dehydrogenase; HDAC1, histone deacetylase 1; HDAC2, histone deacetylase 2; HDAC3, histone deacetylase 3; HDAC4, histone deacetylase 4; HDAC5, histone deacetylase 5; HDAC6, histone deacetylase 6; p-HDAC, phosphorylated form of HDAC.

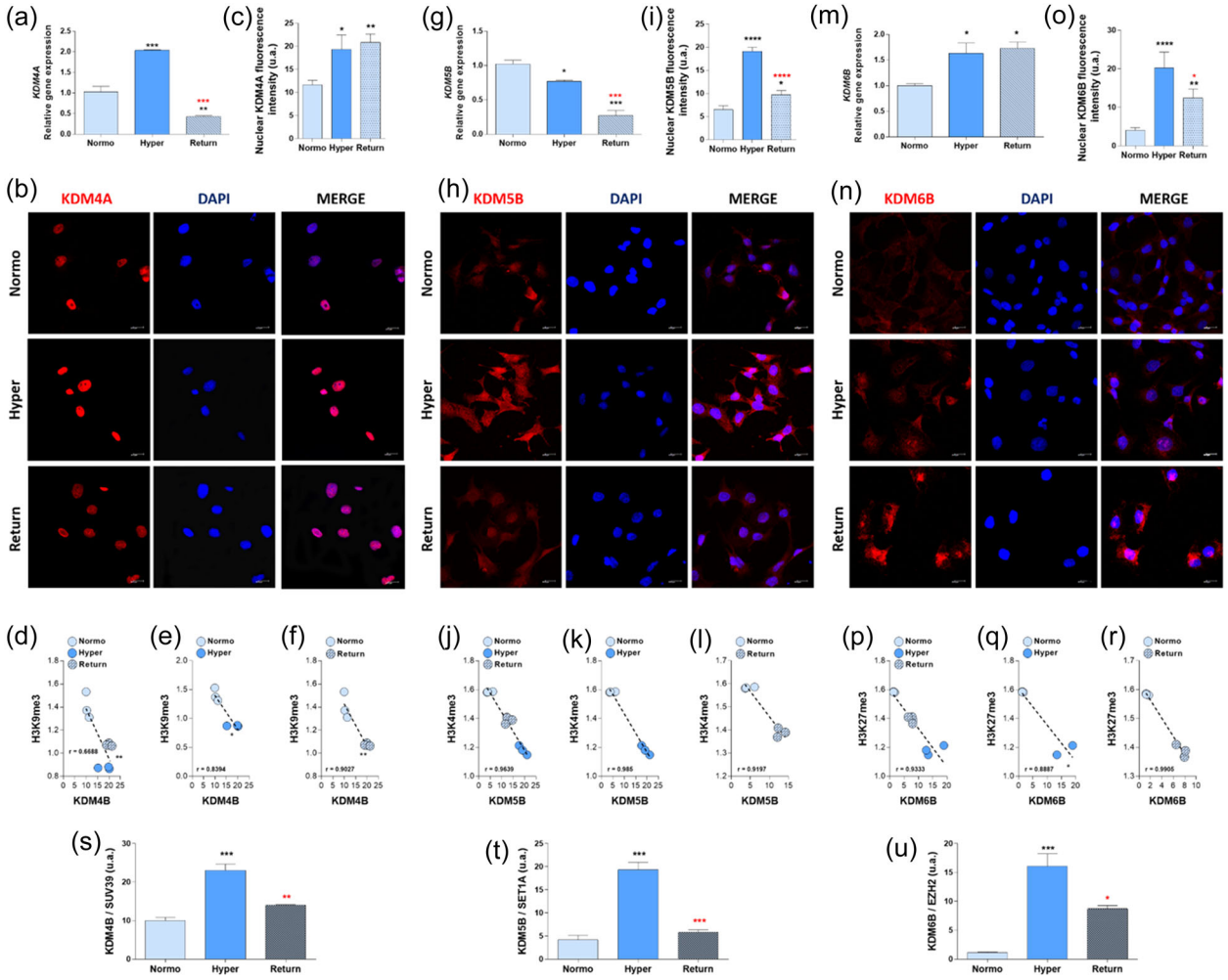

FIGURE 3 Gene expression and subcellular localization patterns of constituents with the same function but distinct substrate affinities. Gene expression analysis of members with affinity to H3K9me3, H3K4me3, and H3K27me3 Substrates (KDM4A, KDM5B, and KDM6B) by qPCR, Normalized to 18S, β-ACTIN, and GAPDH expression, and expressed as mean ± standard deviation of three independent experiments (a, g, n). The intensity of nuclear fluorescence of KDM4A, KDM5B, and KDM6B protein was determined using a LAS AF program (c, i, p) and images of fluorescence confocal microscopy are representative of three independent experiments and shows the subcellular distribution of KDM4A (b), KDM5B (h), and KDM6B (o) proteins. Correlation analyzes with the Pearson product moment between the methylation level of the H3K4me3 (d–f), H3K9me3 (j–l), and H3K27me3 (p–r) marks obtained by immunoblotting with the nuclear content of histone demethylase KDMs obtained by confocal microscopy analysis. Graphical representation of the ratio between the protein content of the histones demethylases and histone methylase specific to the marks H3K9me3 (t), H3K4me3 (u), and H3K27me3 (v). The value for Normo condition was normalized to 1 and the relative values obtained to Hyper or Return are shown in fold-changes. Differences were considered statistically significant when $^{*}p < .04$, $^{**}p < .001$, $^{***}p < .0002$, $^{****}p < .0001$ when compared with the control (Normo) group; and $^{*}p < .04$, $^{**}p < .001$, $^{***}p < .0002$, $^{****}p < .0001$ when compared with Hyper group. GAPDH, glyceraldehyde-3-phosphate dehydrogenase; KDM4A, lysine demethylase 4A; KDM5B, lysine demethylase 5B; KDM6B, lysine demethylase 6B.

accessibility (Sterner & Berger, 2000; Zhang et al., 2015). Our observations of decreased acetylation (H3K9Ac, H3K27Ac) and methylation (H3K4me3, H3K27me3) suggest a complex regulation of chromatin architecture in response to shear stress. Histone methylation, while not altering the charge of histone tails, significantly affects their interaction with DNA, with H3K4me3 marking transcriptional activation sites and H3K9 and H3K27me3 signaling repression (Li et al., 2017; Vakoc et al., 2005). Notably, the interaction of H3K9me3 with DNMT1 and the antagonistic effect of H3K4me3 on DNMT3A/B highlight a sophisticated crosstalk between histone methylation and DNA methylation, which is critical for maintaining or altering gene expression patterns (Yinglu et al., 2021).

The decrease in H3K4me3 and H3K27me3, potentially driven by the upregulation of nuclear KDMs in response to oscillatory shear stress, coupled with the downregulation of DNMT3A/B observed in the Return group, suggests an adaptive epigenetic landscape conducive to new methylation patterns, as it is shown by others (Kooistra et al., 2012). These findings shed light to the complexity of transcriptional regulation under mechanical stress, underscored by the nuanced interplay of histone conformations.

Our research builds on existing murine studies that connect shear stress with histone modification-mediated gene expression, such as VEGF activation and alterations in the renin-angiotensin pathway (Gonzalez-Jaramillo et al., 2019; Illi et al., 2005). We extend these insights by delineating a broader spectrum of histone modifications, particularly those occurring through independent pathways, under the influence of oscillatory shear stress.

The genomic landscape of endothelial cells is intricately regulated by the balance between histone methylation and acetylation, governed by the activity of HMTs, HDMs, HATs, and HDACs (Greer & Shi, 2012;

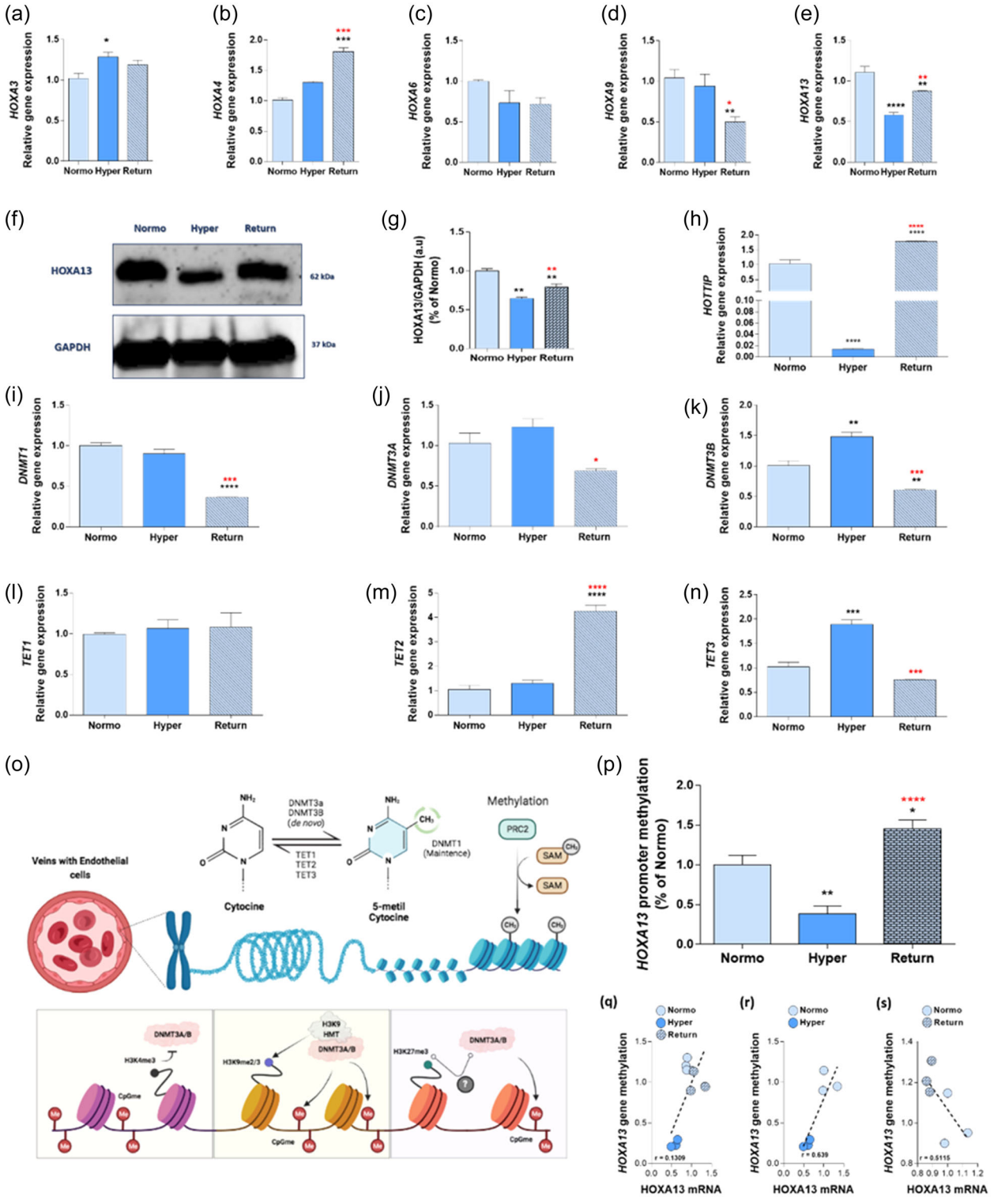

FIGURE 4 (See caption on next page).

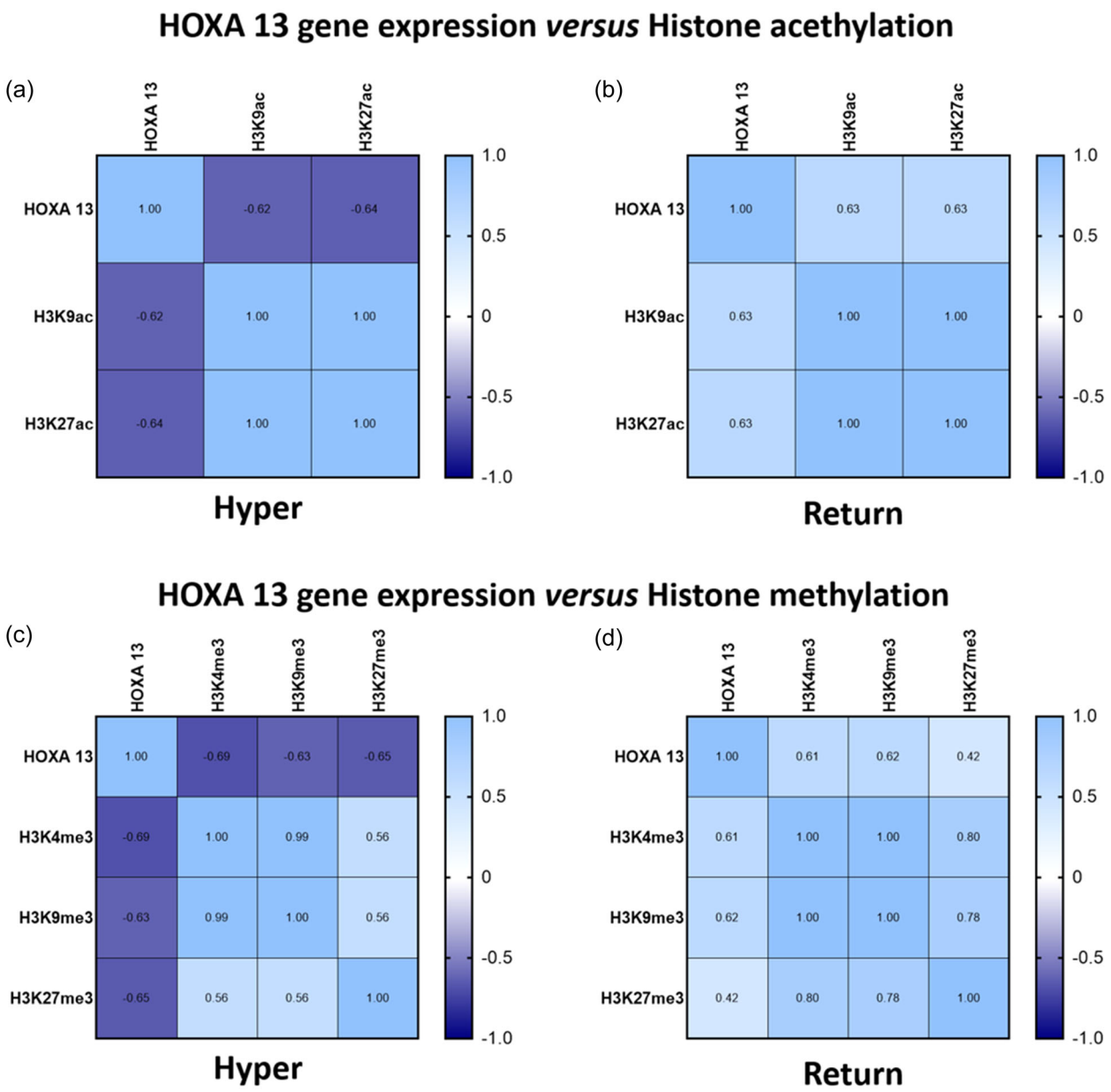

FIGURE 5 Pearson's correlation involving HOXA13 gene expression and epigenetic marks. Pearson correlation analysis between HOXA13 expression and epigenetic marks of acetylation and methylation were performed using correlation matrices. HOXA13 versus histone acetylation (a) Hyper and (b) Return; HOXA13 versus histone methylation (c) Hyper and (d) Return. Significant positive correlation between $r = .683$ and 1.

FIGURE 4 HOX profiles and epigenetic machinery in endothelial cell mechanosignaling. The gene expression of the HOX genes, HOXA3, 4, 6, 9, and 13 were performed by qPCR (a–e). One representative immunoblot of three independent experiments (f) and densitometric analysis (g) revels that HOXA13 also suffered some difference in its protein content. Similar result was observed in the gene expression of the long noncoding RNA HOTTIP (h). Changes in epigenetic machinery genes are observed in gene expression results of DNMTs 1, 3A and 3B (i–k). Difference in qPCR results of some enzymes responsible to remove methylated cytosine, TETs, are observed significant for TET2 and TET3 (l–n). Schematic representation of the interaction between DNA methylation mechanisms and histone changes (o). Methylation level of the HOXA13 promoter region was determined by qPCR through DNA glucosylation T4-BGT, followed by MspI and HpaII digestion (p). The relationship of gene expression and DNA methylation status of HOXA13 genes is shown in a graphical correlation format (q–s). The value for Normo condition was normalized to 1 and the relative values obtained to Hyper or Return are shown in fold-changes. Differences were considered statistically significant when $^{*}p < .04$, $^{**}p < .001$, $^{***}p < .0002$, $^{****}p < .0001$ when compared with the control (Normo) group; and $^{*}p < .04$, $^{**}p < .001$, $^{***}p < .0002$, $^{****}p < .0001$ when compared with Hyper group. All results of gene expression and DNA methylation were expressed as mean ± standard of three independent experiments performed in technical duplicate, normalized by *18S*, *β-ACTIN* and *GAPDH* genes expression level. DNMT1, DNA methyltransferase 1; DNMT3A, DNA methyltransferase 3 alpha; DNMT3B, DNA methyltransferase 3 beta; HOXA3, homeobox A3; HOXA4, homeobox A4; HOXA6, homeobox A6; HOXA9, homeobox A9; HOXA13, homeobox A13; HOTTIP, HOXA distal transcript antisense RNA; TET1, tet methylcytosine dioxygenase 1; TET2, tet methylcytosine dioxygenase 2; TET3, tet methylcytosine dioxygenase 3.

Trisciuoglio et al., 2018). Our findings indicate a complex relationship between gene expression and the protein levels of these epigenetic regulators, suggesting that the transcriptional inhibition under high shear stress is mediated through a heightened histone demethylation and deacetylation activity. The role of HDACs in endothelial differentiation and the influence of KDM5 family members in maintaining endothelial homeostasis and cell cycle progression highlight the multifaceted nature of these epigenetic mechanisms (Hayami et al., 2010; Mokou et al., 2019; Rössig et al., 2005; Yeh et al., 2019).

In light of the pivotal role of HOX cluster genes in vascular development and endothelial function, our focused analysis on the HOXA cluster genes provides valuable perspectives on their contribution to mechanosignaling (Gorski & Walsh, 2000). Our study specifically investigates HOXA13, known for its essential role in vascular integrity and implicated in placental development and preeclampsia (Shaut et al., 2008a; Stadler et al., 2001; Rambaldi et al., n.d.). We explored the epigenetic regulation of HOXA13 in response to shear stress and, while we found no direct correlation between the methylation status of its promoter and expression, we observed a positive correlation between histone modifications and chromatin structure, reinforcing the notion that epigenetic remodeling is a crucial factor in transcriptional regulation (Jenuwein & Allis, 2001; Narlikar et al., 2002).

The connection between chromatin modifications and transcriptional repression patterns is further supported by the association of HOXA13 with the long noncoding RNA (lncRNA) HOTTIP. Our data, alongside previous studies, suggests that HOTTIP plays a significant role in regulating HOXA gene expression, including HOXA13, through the recruitment of the WDR5/MLL complex (Sang et al., 2016; Wang et al., 2011). This study, therefore, contributes to the expanding understanding of transcriptional regulation within the endothelial context, particularly under the modulating influence of oscillatory shear stress.

Finally, the Figure 6 summarizes the key findings. Overall, this study shows the first demonstration that endothelial cells subjected to laminar shear stress exhibit a significant reduction in HOXA13 protein levels. Additionally, we have shown that the epigenetic landscape of these cells adapts to mechanical stress by modifying histone markers: specifically, there is a decrease in both the methylation levels of H3K27me3 and H3K4me3, as well as the acetylation of K9 and K27 residues. Our data suggest an intricate process of epigenetic regulation, notably histone modification and its consequent effect on chromatin structure and gene expression in endothelial cells under increased shear stress. This study is the inaugural report of the significant role these epigenetic alterations play in modulating HOXA13 gene activity, potentially in concert with the lncRNA HOTTIP. Of course, the implications of these findings extend beyond basic science, underscoring the necessity for advanced preclinical studies to further elucidate the physiological functions of HOXA13 within vascular biology. Such investigations are particularly relevant for

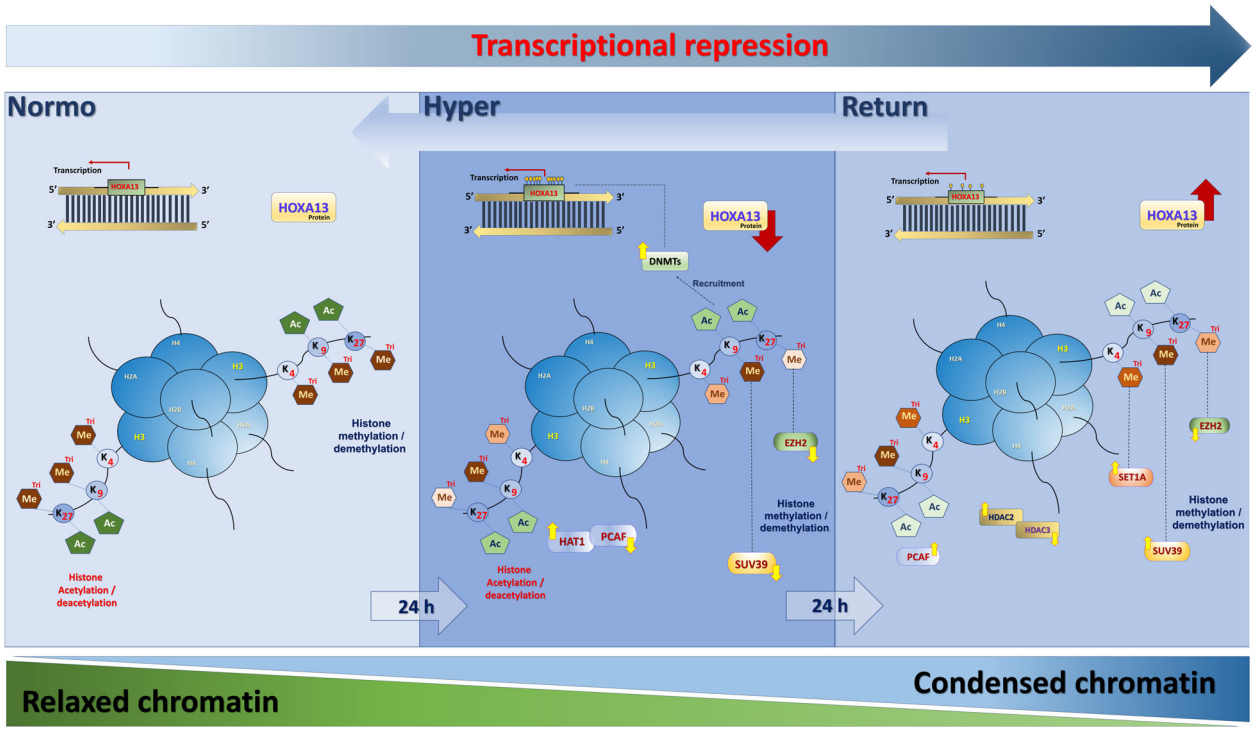

FIGURE 6 Schematic representation of the molecular effects of lamia shear stress on endothelial cells. Here we demonstrate that the laminar mechanical challenge under hypertensive conditions causes changes in the protein content of the acetylation (H3K4Ac, H3K27Ac) and trimethylation (H3K4me3, H3K4me3, and H3K27me3) and HOXA13 protein content, which in turn seems to be mediated by the imbalance of the protein content of the enzymes involved in the acetylation/deacetylation processes (HAT1, PCAF, and HDACs) as well as the enzymes involved in the methylation of lysine residues (SET1A, EZH2, and SUV39).

understanding the pathogenesis of hypertension and could inform the development of novel therapeutic strategies.

AUTHOR CONTRIBUTIONS

Thaís Silva Pinto, Geórgia da Silva Feltran, Célio Júnior da C. Fernandes, Amanda Fantini Camargo Andrade, Simone L. Silva, Abdulwahab A. Abuderman, Willian F. Zambuzzi, and Rodrigo A. Foganholi da Silva made substantial contributions to conception and design, and acquisition of data, and analysis and interpretation of data. Abdulwahab A. Abuderman, Willian F. Zambuzzi, and Rodrigo A. Foganholi da Silva participated in drafting the article and revising it critically for important intellectual content. Thaís Silva Pinto, Geórgia da Silva Feltran, Simone L. Silva, Célio Júnior da C. Fernandes, Amanda Fantini Camargo Andrade, Alex de Camargo Coque, Abdulwahab A. Abuderman, Willian F. Zambuzzi, and Rodrigo A. Foganholi da Silva gave final approval of the version to be submitted and any revised version.

ACKNOWLEDGMENTS

The authors are grateful to Centro de Microscopia Eletrônica, IBB-UNESP, Botucatu-SP, for the confocal microscopy assistance. FAPESP: Fundação de Amparo à Pesquisa do Estado de São Paulo (2014/22689-3; 2016/01139-0; 2017/18349-0), Conselho Nacional de Desenvolvimento Científico e Tecnológico [W.F.Z. (CNPq – Bolsa Produtividade em Pesquisa, 314166/2021-1) and R.A.F.S. (CNPq – Bolsa Produtividade em Pesquisa, 301498/2022-9), and CAPES (Coordenação de Aperfeiçoamento de Pessoal de Nível Superior), code 01.

CONFLICT OF INTEREST STATEMENT

The authors declare no conflicts of interest.

DATA AVAILABILITY STATEMENT

The data that support the findings of this study are available from the corresponding author upon reasonable request. Data will be available upon request to corresponding author.

ORCID

Willian F. Zambuzzi http://orcid.org/0000-0002-4149-5965
Rodrigo A. Foganholi da Silva http://orcid.org/0000-0002-7754-1855

REFERENCES

Accari, S. L., & Fisher, P. R. (2015). Emerging roles of JmjC domain-containing proteins. *Int. Rev. Cell Mol. Biol*, *319*, 165–220. https://doi.org/10.1016/bs.ircmb.2015.07.003

Alberti, K. G. M. M., & Zimmet, P. Z. (1998). Definition, diagnosis and classification of diabetes mellitus and its complications. Part 1: diagnosis and classification of diabetes mellitus provisional report of a WHO consultation. *Diabetic Medicine*, *15*, 539–553. https://doi.org/10.1002/(SICI)1096-9136(199807)15:7<539

Baubec, T., & Schübeler, D. (2014). Genomic patterns and context specific interpretation of DNA methylation. *Current Opinion in Genetics & Development*, *25*, 85–92. https://doi.org/10.1016/j.gde.2013.11.015

Bernatova, I. (2014). Endothelial dysfunction in experimental models of arterial hypertension: Cause or consequence? *BioMed Research International*, *2014*, 1–14. https://doi.org/10.1155/2014/598271

Bokslag, A., van Weissenbruch, M., Mol, B. W., & de Groot, C. J. M. (2016). Preeclampsia; short and long-term consequences for mother and neonate. *Early Human Development*, *102*, 47–50. https://doi.org/10.1016/j.earlhumdev.2016.09.007

Buchanan, C. F., Verbridge, S. S., Vlachos, P. P., & Rylander, M. N. (2014). Flow shear stress regulates endothelial barrier function and expression of angiogenic factors in a 3D microfluidic tumor vascular model. *Cell Adhesion & Migration*, *8*, 517–524. https://doi.org/10.4161/19336918.2014.970001

Cao, K., Collings, C. K., Marshall, S. A., Morgan, M. A., Rendleman, E. J., Wang, L., Sze, C. C., Sun, T., Bartom, E. T., & Shilatifard, A. (2017). SET1A/COMPASS and shadow enhancers in the regulation of homeotic gene expression. *Genes & Development*, *31*, 787–801. https://doi.org/10.1101/gad.294744.116

Chistiakov, D. A., Orekhov, A. N., & Bobryshev, Y. V. (2017). Effects of shear stress on endothelial cells: Go with the flow. *Acta Physiologica*, *219*, 382–408. https://doi.org/10.1111/apha.12725

Cunningham, K. S., & Gotlieb, A. I. (2005). The role of shear stress in the pathogenesis of atherosclerosis. *Laboratory Investigation*, *85*, 9–23. https://doi.org/10.1038/labinvest.3700215

Cuspidi, C., Meani, S., Fusi, V., Severgnini, B., Valerio, C., Catini, E., Leonetti, G., Magrini, F., & Zanchetti, A. (2004). Metabolic syndrome and target organ damage in untreated essential hypertensives. *Journal of Hypertension*, *22*, 1991–1998. https://doi.org/10.1097/00004872-200410000-00023

Delcuve, G. P., Rastegar, M., & Davie, J. R. (2009). Epigenetic control. *Journal of Cellular Physiology*, *219*, 243–250. https://doi.org/10.1002/jcp.21678

Dong, X., & Weng, Z. (2013). The correlation between histone modifications and gene expression. *Epigenomics*, *5*, 113–116. https://doi.org/10.2217/epi.13.13

Du, Y., Liu, Z., Cao, X., Chen, X., Chen, Z., Zhang, X., Zhang, X., & Jiang, C. (2017). Nucleosome eviction along with H3K9ac deposition enhances Sox2 binding during human neuroectodermal commitment. *Cell Death & Differentiation*, *24*, 1121–1131. https://doi.org/10.1038/cdd.2017.62

Esler, M., Eikelis, N., Schlaich, M., Lambert, G., Alvarenga, M., Kaye, D., El-Osta, A., Guo, L., Barton, D., Pier, C., Brenchley, C., Dawood, T., Jennings, G., & Lambert, E. (2008). Human sympathetic nerve biology: Parallel influences of stress and epigenetics in essential hypertension and panic disorder. *Annals of the New York Academy of Sciences*, *1148*, 338–348. https://doi.org/10.1196/annals.1410.064

Expert Panel on Detection, Evaluation, and Treatment of High Blood Cholesterol in Adults (2001). Executive summary of the third report of the national cholesterol education program (NCEP) expert panel on detection, evaluation, and treatment of high blood cholesterol in adults (Adult Treatment Panel III). *JAMA: The Journal of the American Medical Association*, *285*, 2486–2497. https://doi.org/10.1001/jama.285.19.2486.

Félétou, M., Köhler, R., & Vanhoutte, P. M. (2010). Endothelium-derived vasoactive factors and hypertension: Possible roles in pathogenesis and as treatment targets. *Current Hypertension Reports*, *12*, 267–275. https://doi.org/10.1007/s11906-010-0118-2

Fleming, I. (2010). Molecular mechanisms underlying the activation of eNOS. *Pflügers Archiv - European Journal of Physiology*, *459*, 793–806. https://doi.org/10.1007/s00424-009-0767-7

Gomes, A. M., Pinto, T. S., da Costa Fernandes, C. J., da Silva, R. A., & Zambuzzi, W. F. (2020). Wortmannin targeting phosphatidylinositol 3-kinase suppresses angiogenic factors in shear-stressed endothelial cells. *Journal of Cellular Physiology*, *235*(6), 5256–5269. https://doi.org/10.1002/jcp.29412

Gonzalez-Jaramillo, V., Portilla-Fernandez, E., Glisic, M., Voortman, T., Bramer, W., Chowdhury, R., Roks, A. J. M., Jan Danser, A. H.,

Muka, T., Nano, J., & Franco, O. H. (2019). The role of DNA methylation and histone modifications in blood pressure: A systematic review. *Journal of Human Hypertension*, *33*(10), 703–715. https://doi.org/10.1038/s41371-019-0218-7 Epub 2019 Jul 2

Gorski, D. H., & Walsh, K. (2000). The role of homeobox genes in vascular remodeling and angiogenesis. *Circulation Research*, *87*, 865–872. https://doi.org/10.1161/01.res.87.10.865

Greer, E. L., & Shi, Y. (2012). Histone methylation: A dynamic mark in health, disease and inheritance. *Nature Reviews Genetics*, *13*, 343–357. https://doi.org/10.1038/nrg3173

Grundy, S. M., Brewer, Jr., H. B., Cleeman, J. I., Smith, Jr., SC, & Lenfant, C. (2004). Definition of metabolic syndrome: Report of The National Heart, Lung, and Blood Institute/American Heart Association conference on scientific issues related to definition. *Arteriosclerosis, Thrombosis, and Vascular Biology*, *24*, 13–18. https://doi.org/10.1161/01.ATV.0000111245.75752.C6

Guerrero-Romero, F., & Rodríguez-Morán, M. (2005). Concordance between the 2005 international diabetes federation definition for diagnosing metabolic syndrome with The National cholesterol education program adult treatment panel III and the World Health Organization definitions. *Diabetes Care*, *28*, 2588a–2589a. https://doi.org/10.2337/diacare.28.10.2588a

Hayami, S., Yoshimatsu, M., Veerakumarasivam, A., Unoki, M., Iwai, Y., Tsunoda, T., Field, H. I., Kelly, J. D., Neal, D. E., Yamaue, H., Ponder, B. A. J., Nakamura, Y., & Hamamoto, R. (2010). Over-expression of the JmjC histone demethylase KDM5B in human carcinogenesis: Involvement in the proliferation of cancer cells through the E2F/RB pathway. *Molecular cancer*, *9*, 59.

Hrycaj, S. M., & Wellik, D. M. (2016). Hox genes and evolution. *F1000Research*, *5*, 859. https://doi.org/10.12688/f1000research.7663.1

Huynh, Q. K., & McKinsey, T. A. (2006). Protein kinase D directly phosphorylates histone deacetylase 5 via a random sequential kinetic mechanism. *Archives of Biochemistry and Biophysics*, *450*, 141–148. https://doi.org/10.1016/j.abb.2006.02.014

Illi, B., Nanni, S., Scopece, A., Farsetti, A., Biglioli, P., Capogrossi, M. C., & Gaetano, C. (2003). Shear stress-mediated chromatin remodeling provides molecular basis for flow-dependent regulation of gene expression. *Circulation Research*, *93*, 155–161. https://doi.org/10.1161/01.RES.0000080933.82105.29

Illi, B., Scopece, A., Nanni, S., Farsetti, A., Morgante, L., Biglioli, P., Capogrossi, M. C., & Gaetano, C. (2005). Epigenetic histone modification and cardiovascular lineage programming in mouse embryonic stem cells exposed to laminar shear stress. *Circulation Research*, *96*(5), 501–508. https://doi.org/10.1161/01.RES.0000159181.06379.63

Iring, A., Jin, Y.-J., Albarrán-Juárez, J., Siragusa, M., Wang, S., Dancs, P. T., Nakayama, A., Tonack, S., Chen, M., Künne, C., Sokol, A. M., Günther, S., Martínez, A., Fleming, I., Wettschureck, N., Graumann, J., Weinstein, L. S., & Offermanns, S. (2019). Shear stress-induced endothelial adrenomedullin signaling regulates vascular tone and blood pressure. *Journal of Clinical Investigation*, *129*, 2775–2791. https://doi.org/10.1172/JCI123825

Jenuwein, T., & Allis, C. D. (2001). Translating the histone code. *Science*, *293*, 1074–1080. https://doi.org/10.1126/science.1063127

Johnstone, R. W. (2002). Histone-deacetylase inhibitors: novel drugs for the treatment of cancer. *Nature Reviews Drug Discovery*, *1*, 287–299. https://doi.org/10.1038/nrd772

Kato, N., Loh, M., Takeuchi, F., Verweij, N., Wang, X., Zhang, W., Kelly, T. N., Saleheen, D., Lehne, B., Leach, I. M., Drong, A. W., Abbott, J., Wahl, S., Tan, S.-T., Scott, W. R., Campanella, G., Chadeau-Hyam, M., Afzal, U., Ahluwalia, T. S., … Chambers, J. C. (2015). Trans-ancestry genome-wide association study identifies 12 genetic loci influencing blood pressure and implicates a role for DNA methylation. *Nature Genetics*, *47*, 1282–1293. https://doi.org/10.1038/ng.3405

Kooistra, S. M., Helin, K., Helin, K. (2012). Molecular mechanisms and potential functions of histone demethylases. *Nature Reviews Molecular Cell Biology*, *13*(5), 297–311. https://doi.org/10.1038/nrm3327

Lee, D.-Y., Lee, C.-I., Lin, T.-E., Lim, S. H., Zhou, J., Tseng, Y.-C., Chien, S., & Chiu, J.-J. (2012a). Role of histone deacetylases in transcription factor regulation and cell cycle modulation in endothelial cells in response to disturbed flow. *Proceedings of the National Academy of Sciences of the United States of America*, *109*, 1967–1972. https://doi.org/10.1073/pnas.1121214109

Lee, H.-A., Cho, H.-M., Lee, D.-Y., Kim, K.-C., Han, H. S., & Kim, I. K. (2012b). Tissue-specific upregulation of angiotensin-converting enzyme 1 in spontaneously hypertensive rats through histone code modifications. *Hypertens. (Dallas, Tex. 1979)*, *59*, 621–626. https://doi.org/10.1161/HYPERTENSIONAHA.111.182428.

Levy, E., Spahis, S., Bigras, J.-L., Delvin, E., & Borys, J.-M. (2017). The epigenetic machinery in vascular dysfunction and hypertension. *Current Hypertension Reports*, *19*, 52. https://doi.org/10.1007/s11906-017-0745-y

Li, Y.-N., Sheng, M.-Y., Yang, F.-C., & Zhou, Y. (2017). Role of histone methylation in myeloid malignancies—Review. *Zhongguo shi yan xue ye xue za zhi*, *25*, 235–239.

Lu, Q. (2013). The critical importance of epigenetics in autoimmunity. *Journal of Autoimmunity*, *41*, 1–5. https://doi.org/10.1016/j.jaut.2013.01.010

McCabe, M. T., Graves, A. P., Ganji, G., Diaz, E., Halsey, W. S., Jiang, Y., Smitheman, K. N., Ott, H. M., Pappalardi, M. B., Allen, K. E., Chen, S. B., Della Pietra, 3rd, A., Dul, E., Hughes, A. M., Gilbert, S. A., Thrall, S. H., Tummino, P. J., Kruger, R. G., Brandt, M., … Creasy, C. L. (2012). Mutation of A677 in histone methyltransferase EZH2 in human B-cell lymphoma promotes hypertrimethylation of histone H3 on lysine 27 (H3K27). *Proceedings of the National Academy of Sciences*, *109*, 2989–2994. https://doi.org/10.1073/pnas.1116418109

Mokou, M., Klein, J., Makridakis, M., Bitsika, V., Bascands, J.-L., Saulnier-Blache, J. S., Mullen, W., Sacherer, M., Zoidakis, J., Pieske, B., Mischak, H., Roubelakis, M. G., Schanstra, J. P., & Vlahou, A. (2019). Proteomics based identification of KDM5 histone demethylases associated with cardiovascular disease. *EBioMedicine*, *41*, 91–104. https://doi.org/10.1016/j.ebiom.2019.02.040

Mu, S., Shimosawa, T., Ogura, S., Wang, H., Uetake, Y., Kawakami-Mori, F., Marumo, T., Yatomi, Y., Geller, D. S., Tanaka, H., & Fujita, T. (2011). Epigenetic modulation of the renal β-adrenergic–WNK4 pathway in salt-sensitive hypertension. *Nature Medicine*, *17*, 573–580. https://doi.org/10.1038/nm.2337

Myers, C., Charboneau, A., & Boudreau, N. (2000). Homeobox B3 promotes capillary morphogenesis and angiogenesis. *The Journal of Cell Biology*, *148*, 343–352. https://doi.org/10.1083/jcb.148.2.343

Narlikar, G. J., Fan, H.-Y., & Kingston, R. E. (2002). Cooperation between complexes that regulate chromatin structure and transcription. *Cell*, *108*, 475–487. https://doi.org/10.1016/s0092-8674(02)00654-2

dela Paz, N. G., Walshe, T. E., Leach, L. L., Saint-Geniez, M., & D'Amore, P. A. (2012). Role of shear-stress-induced VEGF expression in endothelial cell survival. *Journal of Cell Science*, *125*, 831–843. https://doi.org/10.1242/jcs.084301

Pinto, T. S., Fernandes, C., da Silva, R. A., Gomes, A. M., Vieira, J. C. S., Padilha, P. M., & Zambuzzi, W. F. (2019). c-Src kinase contributes on endothelial cells mechanotransduction in a heat shock protein 70-dependent turnover manner. *Journal of cellular physiology*, *234*, 11287–11303. https://doi.org/10.1002/jcp.27787

Pinto, T. S., Fernandes, C. J. C., da Silva, R. A., Gomes, A. M., Vieira, J. C. S., Padilha, P. M., & Zambuzzi, W. F. (2019). c-Src kinase contributes on endothelial cells mechanotransduction in a heat shock protein 70-dependent turnover manner. *Journal of Cellular Physiology*, Jul *234*(7), 11287–11303. https://doi.org/10.1002/jcp.27787

Pojoga, L. H., Williams, J. S., Yao, T. M., Kumar, A., Raffetto, J. D., do Nascimento, G. R. A., Reslan, O. M., Adler, G. K., Williams, G. H., Shi, Y., & Khalil, R. A. (2011). Histone demethylase LSD1 deficiency

during high-salt diet is associated with enhanced vascular contraction, altered NO-cGMP relaxation pathway, and hypertension. *American Journal of Physiology-Heart and Circulatory Physiology*, *301*, H1862–H1871. https://doi.org/10.1152/ajpheart.00513.2011

Qin, X., Wang, X., Wang, Y., Tang, Z., Cui, Q., Xi, J., J. Li, Y. S., Chien, S., & Wang, N. (2010). MicroRNA-19a mediates the suppressive effect of laminar flow on cyclin D1 expression in human umbilical vein endothelial cells. *Proceedings of the National Academy of Sciences*, *107*, 3240–3244. https://doi.org/10.1073/pnas.0914882107

Rambaldi, M. P., Pieralli, A., Ottanelli, S., Serena, C., Simeone, S., Mello, G., & Mecacci, F. (n.d.) OS086. Methylation status of the HOXA13 promoter region in placental tissue of pregnancies complicated by early onset severe preeclampsia. *Pregnancy Hypertension: An International Journal of Women's Cardiovascular Health*, *2*(3), 224–225. https://doi.org/10.1016/j.preghy.2012.04.087

Rössig, L., Urbich, C., Brühl, T., Dernbach, E., Heeschen, C., Chavakis, E., Sasaki, K., Aicher, D., Diehl, F., Seeger, F., Potente, M., Aicher, A., Zanetta, L., Dejana, E., Zeiher, A. M., & Dimmeler, S. (2005). Histone deacetylase activity is essential for the expression of HoxA9 and for endothelial commitment of progenitor cells. *The Journal of Experimental Medicine*, *201*, 1825–1835. https://doi.org/10.1084/jem.20042097

de Ruijter, A. J. M., Gennip, A. H., Caron, H. N., Kemp, S., & Kuilenburg, A. B. P. (2003). Histone deacetylases (HDACs): Characterization of the classical HDAC family. *Biochemical Journal*, *370*, 737–749. https://doi.org/10.1042/BJ20021321

Sang, Y., Zhou, F., Wang, D., Bi, X., Liu, X., Hao, Z., Li, Q., & Zhang, W. (2016). Up-regulation of long non-coding HOTTIP functions as an oncogene by regulating HOXA13 in non-small cell lung cancer. *American Journal of Translational Research*, *8*, 2022–2032.

Schillaci, G., Pirro, M., Vaudo, G., Gemelli, F., Marchesi, S., Porcellati, C., & Mannarino, E. (2004). Prognostic value of the metabolic syndrome in essential hypertension. *Journal of the American College of Cardiology*, *43*, 1817–1822. https://doi.org/10.1016/j.jacc.2003.12.049

Shaut, C. A., Keene, D. R., Sorensen, L. K., Li, D. Y., & Stadler, H. S. (2008b). HOXA13 is essential for placental vascular patterning and labyrinth endothelial specification. *PLoS Genetics*, *4*(5), e1000073. https://doi.org/10.1371/journal.pgen.1000073

Shaut, C. A. E., Keene, D. R., Sorensen, L. K., Li, D. Y., & Stadler, H. S. (2008a). HOXA13 is essential for placental vascular patterning and labyrinth endothelial specification. *PLoS Genet*, *4*, e1000073. https://doi.org/10.1371/journal.pgen.1000073

da Silva, R. A., Fernandes, C. J. C., Feltran, G. S., Gomes, A. M., de Camargo Andrade, A. F., Andia, D. C., Peppelenbosch, M. P., & Zambuzzi, W. F. (2019). Laminar shear stress-provoked cytoskeletal changes are mediated by epigenetic reprogramming of TIMP1 in human primary smooth muscle cells. *Journal of Cellular Physiology*, *234*, 6382–6396. https://doi.org/10.1002/jcp.27374

da Silva, R. A., Ferreira, M. R., Gomes, A. M., & Zambuzzi, W. F. (2020). LncRNA HOTAIR is a novel endothelial mechanosensitive gene. *Journal of Cellular Physiology*, May *235*(5), 4631–4642. https://doi.org/10.1002/jcp.29340

Simon, P. H. G., Sylvestre, M.-P., Tremblay, J., & Hamet, P. (2016). Key considerations and methods in the study of gene-environment interactions. *American Journal of Hypertension*, *29*, 891–899. https://doi.org/10.1093/ajh/hpw021

Stadler, H. S., Higgins, K. M., & Capecchi, M. R. (2001). Loss of Eph-receptor expression correlates with loss of cell adhesion and chondrogenic capacity in Hoxa13 mutant limbs. *Development*, *128*, 4177–4188.

Sterner, D. E., & Berger, S. L. (2000). Acetylation of histones and transcription-related factors. *Microbiology and Molecular Biology Reviews*, *64*, 435–459. https://doi.org/10.1128/mmbr.64.2.435-459.2000

Tremblay, J. C., Thom, S. R., Yang, M., & Ainslie, P. N. (2017). Oscillatory shear stress, flow-mediated dilatation, and circulating microparticles at sea level and high altitude. *Atherosclerosis*, *256*, 115–122. https://doi.org/10.1016/j.atherosclerosis.2016.12.004

Trisciuoglio, D., Di Martile, M., & Del Bufalo, D. (2018). Emerging role of histone acetyltransferase in stem cells and cancer. *Stem Cells International*, *2018*, 1–11. https://doi.org/10.1155/2018/8908751

Udali, S., Guarini, P., Moruzzi, S., Choi, S.-W., & Friso, S. (2013). Cardiovascular epigenetics: From DNA methylation to microRNAs. *Molecular Aspects of Medicine*, *34*, 883–901. https://doi.org/10.1016/j.mam.2012.08.001

Untergasser, A., Cutcutache, I., Koressaar, T., Ye, J., Faircloth, B. C., Remm, M., & Rozen, S. G. (2012). Primer3–new capabilities and interfaces. *Nucleic Acids Research*, *40*, e115. https://doi.org/10.1093/nar/gks596

Vakoc, C. R., Mandat, S. A., Olenchock, B. A., & Blobel, G. A. (2005). Histone H3 lysine 9 methylation and HP1γ are associated with transcription elongation through mammalian chromatin. *Molecular Cell*, *19*, 381–391. https://doi.org/10.1016/j.molcel.2005.06.011

Verreault, A., Kaufman, P. D., Kobayashi, R., & Stillman, B. (1998). Nucleosomal DNA regulates the core-histone-binding subunit of the human Hat1 acetyltransferase. *Current Biology*, *8*, 96–108.

Wang, K. C., Yang, Y. W., Liu, B., Sanyal, A., Corces-Zimmerman, R., Chen, Y., Lajoie, B. R., Protacio, A., Flynn, R. A., Gupta, R. A., Wysocka, J., Lei, M., Dekker, J., Helms, J. A., & Chang, H. Y. (2011). A long noncoding RNA maintains active chromatin to coordinate homeotic gene expression. *Nature*, *472*, 120–124. https://doi.org/10.1038/nature09819

Wierda, R. J., Rietveld, I. M., van Eggermond, M. C. J. A., Belien, J. A. M., van Zwet, E. W., Lindeman, J. H. N., & van den Elsen, P. J. (2015). Global histone H3 lysine 27 triple methylation levels are reduced in vessels with advanced atherosclerotic plaques. *Life Sciences*, *129*, 3–9. https://doi.org/10.1016/j.lfs.2014.10.010

Yeh, I. J., Esakov, E., Lathia, J. D., Miyagi, M., Reizes, O., & Montano, M. M. (2019). Phosphorylation of the histone demethylase KDM5B and regulation of the phenotype of triple negative breast cancer. *Scientific reports*, *9*(1), 17663.

Yoon, K.-A., Hwangbo, B., Kim, I.-J., Park, S., Kim, H. S., Kee, H. J., Lee, J. E., Jang, Y. K., Park, J.-G., & Lee, J. S. (2006). Novel polymorphisms in the SUV39H2 histone methyltransferase and the risk of lung cancer. *Carcinogenesis*, *27*, 2217–2222. https://doi.org/10.1093/carcin/bgl084

Zhang, Y.-X., Sun, H.-L., Liang, H., Li, K., Fan, Q.-M., & Zhao, Q.-H. (2015). Dynamic and distinct histone modifications of osteogenic genes during osteogenic differentiation. *Journal of Biochemistry*, *158*, 445–457. https://doi.org/10.1093/jb/mvv059

Zhong, J., Eliceiri, B., Stupack, D., Penta, K., Sakamoto, G., Quertermous, T., Coleman, M., Boudreau, N., & Varner, J. A. (2003). Neovascularization of ischemic tissues by gene delivery of the extracellular matrix protein Del-1. *Journal of Clinical Investigation*, *112*, 30–41. https://doi.org/10.1172/JCI17034

SUPPORTING INFORMATION

Additional supporting information can be found online in the Supporting Information section at the end of this article.

How to cite this article: Pinto, T. S., Feltran, G. d. S., Fernandes, C. J. d. C., Camargo Andrade, A. F. d., Coque, A. d. C., Silva, S. L., Abuderman, A. A., Zambuzzi, W. F., & Foganholi da Silva, R. A. (2024). Epigenetic changes in shear-stressed endothelial cells. *Cell Biology International*, *48*, 665–681. https://doi.org/10.1002/cbin.12138